Experimental Study on the Discharge Coefficient of Triangular Piano Key Side Weirs with Different Geometries

Maryam Yeganeh[1], Mohammadreza Jalili Ghazizadeh[2*], Mojtaba Saneie[3], Ehsanollah Zeighami[1]

[1] Department of Civil Engineering, Arak Branch, Islamic Azad University, Arak, Iran
[2] Department of Civil, Water and Environmental Engineering, Shahid Beheshti University, Tehran, Iran
[3] Soil Conservation and Watershed Management Research Institute, Agricultural Research, Education and Extension Organization, Tehran, Iran

* m_jalili@sbu.ac.ir

Abstract

The piano key side weir is introduced as a new hydraulic structure to improve the outflow performance where the opening length of distribution channels is restricted. This study used 370 high-resolution tests on three linear and 24 triangular piano key side weirs. The study experimentally investigates the effects of different upstream angles on the discharge coefficient of the triangular piano key side weirs with various geometries. In these tests, continuous improvement has been achieved by reducing the ratio of upstream angles for triangular piano key side weirs with the same crest length. The estimation of discharge coefficients using De Marchi's equation shows an average increase of 7.2% to 17% for the triangular piano key side weirs, considering the variation of upstream angles. The data analysis shows that the deflection angles of triangular piano key side weirs are also vital for outflow efficiency. A new reliable equation is proposed to estimate the discharge coefficient of piano key side weirs based on some dimensionless parameters (different ratios of upstream angles (δ_1/δ_2), dimensionless weir length (L/W), dimensionless weir height (h_1/P), dimensionless overhang length (h_1/B_i), and the downstream Froude number (F_2). Also, the statistical indices were used to evaluate the precision of the nonlinear equation for triangular piano key side weirs. The R^2 and MAE for 70% of the experimental data were 0.91 and 0.052, respectively.

Keywords:

Piano key side weirs, upstream angles, different geometry, triangular side weirs, discharge coefficient

1. Introduction

The common usage of side weirs as a control structure is evident in irrigation systems, drainage channels, hydropower facilities, wastewater plants, and urban sewage systems. Non-uniform flows are categorized into rapidly varied flows and gradually varied flows. Studies have been conducted on the rapidly varied flows [1]. For analysis of flow over side weirs, spatially varied flow (SVF) with decreasing discharge is considered [2]. For this type of flow, the pressure is hydrostatic, and the bottom slope of the main channel is usually small [2, 3]. Applying the constant energy assumption implies that the longitudinal velocity component of flow at any section equals the average flow velocity in the main channel. Therefore, the variation of energy in the channel, apart from frictional losses, remains constant. De Marchi proposed an analytical equation to analyze side weir flow using the hypothesis of constant specific energy along the side weir [4]. Accordingly, many studies have been conducted on side weirs to find De Marchi's discharge coefficient with both experimental and numerical perspectives [5-9]. In the literature, the linear sharp-edged side weirs were the primary concern of some researchers ([10-16]). It has been shown that the velocity distribution was significantly affected near the linear sharp-edged side weirs [5]. The effects of hydraulic and geometric parameters of the channel and side weir shape on the discharge coefficient were studied in a subcritical flow [8]. The hydraulic properties of linear sharp-edged side weirs were studied in arched channels with a 180-degree arc [10]. The water surface in linear side weirs was examined by modifying the side weir geometry [15]. An equation for predicting the discharge coefficient of linear side weirs in an earthen channel for the subcritical flow regime was proposed [16].

In the channel bank, the limited opening length reduces the flow rate on the linear side weir. Therefore, the labyrinth side weir can be replaced with an elongated crest length to enhance the discharge capacity. Several studies have been published on the discharge coefficient of labyrinth side weirs ([17-24]). It has been shown that discharge coefficients for the triangular labyrinth side weirs were higher than for linear side weirs [18]. Evaluating the discharge capacity of the triangular labyrinth side weirs with one, two, and four cycles showed that the efficiency of single and double-

labyrinth side weirs is better than four-labyrinth side weirs in the subcritical flow regime [21]. The trapezoidal side weir's efficiency was better than the triangular side weir due to the shorter length of the disturbance wedge in a subcritical flow regime [22]. A research result indicated that the efficiency of asymmetric triangular labyrinth side weirs is better than symmetric ones with the same crest length [23]. Compared with F_2 (Froude number at the downstream end of the side weir), the better correlation between the discharge coefficient of these side weirs and F_1 (Froude number at the upstream end of the side weir) was represented. The Finite Volume Method was used to investigate the effects of different numbers of teeth on one-cycle sharp-edged triangular weirs, considering the amount of various angles of the weir tip [24].

A piano key weir (PKW) has one main advantage over a labyrinth weir. The footprint of the PKW with the same crest length is smaller than the labyrinth weir. Therefore, it is a more efficient alternative in places with a limited footprint. The higher hydraulic performance and economic efficiency are the advantages of the PKWs [25]. In recent years, there have been many studies on various aspects of the PKWs located in the front of the flow in straight channels ([26-31]). Most studies have analyzed the flow over rectangular PKWs, while trapezoidal PKWs have been the subject of some studies. Studying the hydraulic of PKWs showed that PKWs were slightly more efficient than the corresponding rectangular labyrinth side weirs with the same opening length [27]. The discharge coefficient of trapezoidal PKWs was higher than rectangular PKWs [28]. Criteria for the design of trapezoidal PKWs were also proposed based on quantitative analysis for three flow regimes (nappe, transitional, and submerged flow). The relationship between the discharge coefficient and dimensionless parameters was evaluated in type B-PKW and linear weirs [29]. The findings by sensitivity analysis indicated that weir length, water depth, and Froude number are more vital than other dimensionless parameters. The efficiency of a PKW was better than that of a rectangular labyrinth weir [31]. Also, the sloped floor in the input and output cycles of rectangular PKWs reduces the flow contraction rather than the rectangular labyrinth weir.

The literature review shows that some investigations have been reported on PKWs in lateral configuration. Some researchers have studied the performance of piano key side weir (PKSW) [32-

36]. The hydraulic performance of rectangular PKSWs compared with the labyrinth and linear side weirs has been examined [32]. The results showed that the PKSWs have a higher discharge coefficient than the linear side weirs, while there was no significant difference compared with the rectangular labyrinth side weirs. The number of cycles on the efficiency of the type-A trapezoidal PKSW showed that the efficiency of single-PKSWs is better than that of double-PKSWs in a curved channel [33]. The discharge coefficient of trapezoidal PKSWs was 1.2 and 1.87 times higher than that of trapezoidal labyrinth weirs with 12° and 6° sidewall angles, respectively, and 1.5 times higher than triangular labyrinth weirs [34]. Investigating the various schemes of the triangular labyrinth and the type-C piano key side weirs showed continuous improvement by adding sloped floors to the input and output cycles, adding apex overhang to the downstream cycles, and changing a symmetric to an asymmetric plan [35].

Despite the investigations conducted on piano key weirs in frontal configuration and only a few works in lateral configuration, more research on piano key side weirs with various plans is required. Considering the flow direction from the main channel to the lateral channel, it should be necessary to evaluate the effectiveness of the piano key side weirs with different plans that can affect the discharge coefficient. The upstream angles and overhang length are effective parameters on the triangular piano key (TPK) side weir, which has not been comprehensively investigated in previous studies. Rectangular and triangular PKWs are particular types of trapezoidal PKWs, respectively, with $W_i+W_o/w = 1$ and $W_i+W_o/w = 0$, where W_i is the width of the input cycle, W_o is the width of the output cycle, and w is the width of one cycle. This study compared triangular piano key side weirs ($W_i+W_o/w = 0$) with different geometries to achieve a more effective plan design.

The main objectives of this paper are:

(1) To compare the effect of different geometric and hydraulic parameters on the triangular piano key side weirs, including dimensionless weir length (L/W), the dimensionless weir height (h_1/P), the dimensionless weir overhang (h_1/B_i), the upstream angle of the triangular piano key side weir (δ_1/δ_2), and the Froude number at the downstream (F_2);

(2) To find the optimum shape for triangular piano key side weirs to pass the maximum discharge considering the same crest length;

(3) To present a novel relation for triangular piano key side weirs with different upstream angles. (This new relation, which we believe will significantly contribute to the field, is a result of our rigorous research and analysis.)

2. Theoretical Consideration

The equation of a spatially varied flow with descending discharge over a side weir is defined as Eq. 1. In this equation, the pressure distribution is assumed hydrostatic, and the channel is prismatic with no slope. Flow is considered steady and one-dimensional. In this case, if dQ/dx = 0, where there is no decrease in the flow rate, it will be returned to the dynamic equation of gradually varied flow.

$$\frac{dy}{dx} = \frac{S_0 - S_f - \left(\frac{\alpha Q}{gA^2}\right)\left(\frac{dQ}{dx}\right)}{1 - \left(\frac{\alpha Q^2 b}{gA^3}\right)} \quad (1)$$

where y is the water depth in the main channel (variable in the direction of flow); x is the distance in the longitudinal direction; S_0 and S_f are the bottom and friction slopes in the main channel; b is the width of the channel; α is the kinetic energy correction coefficient; Q is the flow discharge in the channel; A is the cross-sectional area of the flow; and g is the gravitational acceleration.

Assuming that S_0 - S_f = 0 (i.e., constant specific energy across the weir) and α = 1, the discharge over the side weir based on the opening length (W) is evaluated using the classic sharp-edged weir formula:

$$Q_w = \frac{2}{3} C_{dw} W \sqrt{2g} (y_1 - P)^{1.5} \quad (2)$$

where Q_w is total discharge over the side weir; C_{dw} is the discharge coefficient of the side weir; y_1 is the water depth at the upstream end of the side weir in the main channel; and P is the weir height. Eq.

(2) has been used to compare the C_{dw} values of linear and piano key side weirs, considering their equal opening lengths in the study.

Regarding the De Marchi hypothesis, the differential equation of spatially varied flow with decreasing discharge can be solved as [4]:

$$x = \frac{3}{2}\frac{b}{C_{dw}}\Phi\left(y, E, P\right) + Const, \quad (3)$$

Here, E is specific energy, and Φ is the De Marchi function defined as:

$$\Phi(y, E, P) = \frac{2E - 3P}{E - P}\sqrt{\frac{E - y}{y - P}} - 3\sin^{-1}\sqrt{\frac{E - y}{E - P}} \quad (4)$$

Applying Eq. (3) at the upstream and downstream of the side weirs for the boundary conditions yields:

$$C_{dw} = \frac{3}{2}\frac{b}{W}\left(\Phi_2 - \Phi_1\right) \quad (5)$$

Subscripts 1 and 2 indicate the upstream and downstream ends of the side weir, respectively. The total diverted discharge over the side weir becomes:

$$Q_w = Q_1 - Q_2 \quad (6)$$

where Q_1 and Q_2 are input and output channel discharges, respectively.

3. Dimensional Analysis

The discharge coefficient of a triangular piano key (TPK) side weir is shown as a function of the following parameters:

$$C_{dw} = f_1\left(h, y, V, B_i, W, P, b, \frac{\delta_1}{\delta_2}\mu, \sigma, \rho, g\right) \quad (7)$$

where h is the piezometric head over the side weir; y can be defined as the depth at the upstream and downstream end of the side weir; V can be defined as the mean flow velocity at the upstream and

downstream end of the side weir; B_i is the overhang length; δ_1/δ_2 is the ratio of upstream angles; μ is the fluid dynamic viscosity; σ is the surface tension; and ρ is the mass density of the fluid.

There are 12 variables according to Buckingham's method (π theorem). Nine dimensionless variables are achieved by taking y, V, and σ as the three main variables. Equation (8) can be obtained by combining the variables as:

$$C_{dw} = f_2\left(\frac{L}{W}, \frac{b}{W}, \frac{b}{B_i}, \frac{h}{P}, \frac{h}{B_i}, \sin\left(\frac{\delta_1}{\delta_2}\right), \mathrm{F} = \frac{V}{\sqrt{gy}}, \mathrm{Re}, \mathrm{We}\right) \quad (8)$$

where F is the Froude number, which can be considered at the upstream or downstream, Re and We are the Reynolds number (ratio of inertial force to viscous force) and Weber number (ratio of inertial force to surface tension force), respectively. In a fully turbulent flow, the impact of the viscous force in comparison with the inertial force could be neglected [37]. This study set the nappe height over the side weir at least 3 cm. Thus, the scale effect due to surface tension is imperceptible [38, 39]. Therefore, Re and We numbers should be removed from effective parameters. Also, the value of b was considered constant; consequently, it is dropped from Eq. (8). By eliminating the less effective variables, the parameters for the discharge coefficient of the TPK side weirs can be reported as:

$$C_{dw} = f_2\left(\frac{L}{W}, \frac{h}{P}, \frac{h}{B_i}, \sin\left(\frac{\delta_1}{\delta_2}\right), \mathrm{F} = \frac{V}{\sqrt{gy}}\right) \quad (9)$$

The water flow at the channel's centerline is more uniform than the side of the weir; therefore, the Froude number at the channel centerline can be used at the upstream or downstream end of the side weir. Although in most studies, the effect of the upstream Froude number has been applied to side weir flows, some researchers used the downstream Froude number affected by both upstream and downstream conditions [14, 23]. The present study has used the downstream Froude number as the dimensionless term to analyze the C_{dw} values.

4. Experimental Setup

Side weir experiments were conducted in a rectangular channel with a length of 11 m, a height of 0.6 m, and a width of 0.6 m (Fig. 1(a)). Water was pumped from the main reservoir to the channel in a closed circulation system. A part of the flow in the main channel deviated and entered the lateral channel by reaching the height of the side weir. The remaining discharge in the main channel was transmitted to the final reservoir. A metal screen was also embedded upstream of the main channel to stabilize the inflow turbulence. The flow depth, lateral discharge, and Froude number range were also controlled using a gate at the end of the main channel. A calibrated 90° V-notched weir was installed downstream of the main channel to measure the flow rate at the main channel.

Additionally, the diverted discharge over the side weir was measured by a rectangular weir at the downstream end of the lateral channel. The water depth measurements were conducted along the transverse (z/b) and longitudinal (x/W) axes using a digital depth profiler with $\pm$0.1 mm precision (x and z are the longitudinal distance from the beginning of the side weir and the transverse distance from the side weir, respectively). In a spatially varied flow with decreasing discharge (Fig. 1(b)), when the flow depth at the upstream (y_1) reaches the height of the side weir (P), the flow discharge is diverted over the side weir. The water depth rises along the channel to the end of the side weir in a subcritical flow.

Fig. 2 shows the plan of two-cycle triangular piano key (TPK) side weirs with the location of the measured parameters in the channel centerline. In this paper, triangular piano key side weirs, as shown in Fig. 2, TPK_1 (Fig. 2(a)), TPK_2 (Fig. 2(b)), and TPK_3 (Fig. 2(c)) are studied with different upstream angles. Each cycle of the TPK side weir consists of one input span with two lateral walls and two semi-output spans. The input and output spans are the opening parts to the upstream and downstream sides, respectively, limited by the lateral walls. For the same values of L/W ratio, the TPK_1 and TPK_3 side weirs create a shorter base length (B_b) for the side weir. Therefore, these side weirs are better alternatives than TPK_2 in terms of footprint restrictions. In this study, three linear side weirs, six TPK_1 side weirs, nine TPK_2 side weirs, and nine TPK_3 side weirs were tested. The hydraulic parameters and the measurement ranges are presented in Table 1.

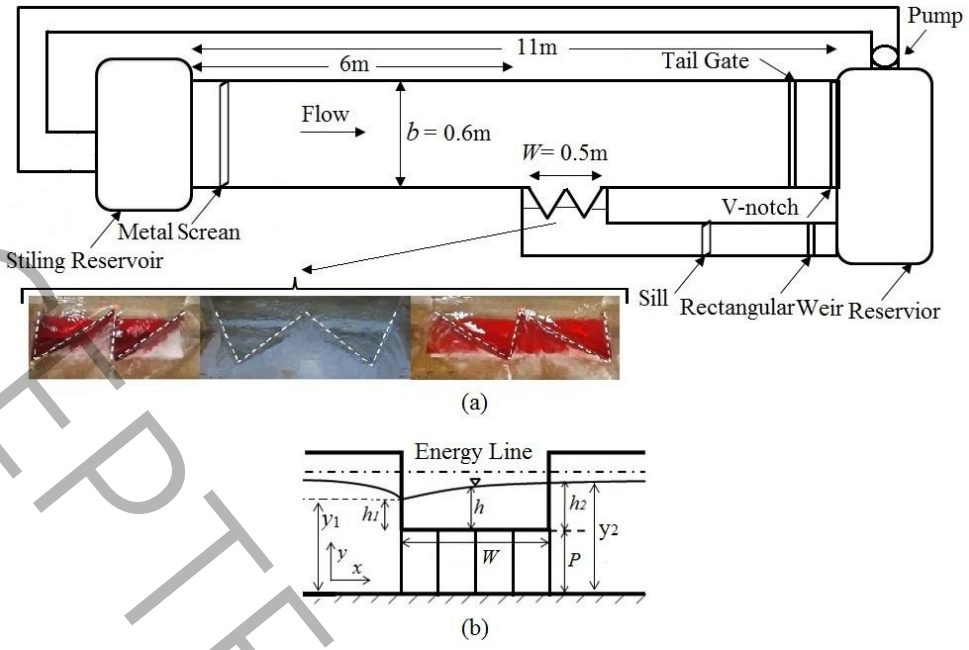

Fig. 1 Experimental set-up: (a) Channel and triangular piano key side weir's plans; (b) Front view of a piano key side weir

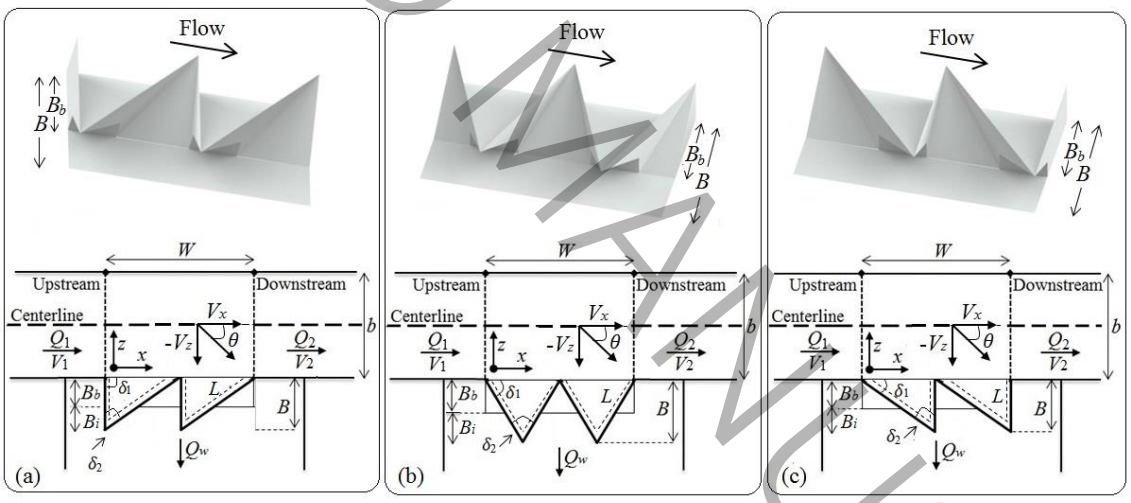

Fig. 2 Geometrical characteristic of tested piano key side weirs: (a) TPK_1; (b) TPK_2; (c) TPK_3

Table 1. Range of variables over the tested weirs

Weir	Runs no.	B (cm)	B_i (cm)	P/B	L/W	h_1/P	F_1	F_2	δ_1/δ_2
Linear	48	-	-	-	-	0.21-1.51	0.08-0.46	0.01-0.27	-
TPK_1	35	17	6.8	0.47,0.7,0.94	1.89	0.31-1.44	0.09-0.55	0.04-0.38	1.61
TPK_1	30	28	11.2	0.29,0.43,0.57	2.6	0.17-1.5	0.14-0.65	0.02-0.41	2.15
TPK_2	48	20	8	0.4,0.6,0.8	1.89	0.23-1.62	0.12-0. 6	0.02-0.43	0.9
TPK_2	42	30	12	0.27,0.4,0.53	2.6	0.19-1.51	0.09-0.73	0.04-0.42	1.5
TPK_2	46	40	16	0.2,0.3,0.4	3.35	0.24-1.26	0. 14-0.76	0.01-0.44	2.07
TPK_3	50	17	6.8	0.47,0.7,0.94	1.89	0.21-1.73	0.09-0.64	0.05-0.3	0.61
TPK_3	35	28	11.2	0.29,0.43,0.57	2.6	0.31-1.45	0.1-0.65	0.08-0.38	1.15
TPK_3	36	38	15.2	0.21,0.32,0.42	3.35	0.24-1.3	0.12-0.73	0.01-0.35	1.7

5. Results and Discussions

The constancy of the energy head along the triangular piano key side weirs was checked using De Marchi's assumption for the computation of the discharge coefficient (C_{dw}). The specific energy loss ($\Delta E = |E_2 - E_1|/E_1$) was calculated at the upstream and downstream of the tested side weirs. The average values were measured as 1.4%, 1.3%, and 1.2% for TPK_1, TPK_2, and TPK_3, respectively. The average values of specific energy for triangular labyrinth side weirs with one and two cycles [17] and with one, two, and four cycles [21] were < 4%, < 4%, 2.1%, 1.7%, and 0.88%, respectively. The results for TPK side weirs are generally acceptable in subcritical flow conditions.

The following experiments have provided a hydraulic comparison between triangular piano key side weirs for subcritical flow conditions. This part compares the efficiency of TPK_1, TPK_2, and TPK_3 side weirs, considering the different ratios of upstream angles. Fig. 3 shows the discharge coefficient (C_{dw}) variation versus the h_1/P for TPK_1, TPK_2, and TPK_3 side weirs with specifications of P = 16 cm and L/W = 1.89 (Fig. 3(a)), P = 12 cm and L/W = 2.6 (Fig. 3(b)). As shown, C_{dw} decreases with the increase of h_1/P. This figure also reveals that the hydraulic performance of the TPK_3 is better than that of the TPK_1 and TPK_2 side weirs, especially for the lower h_1/P values. The average increase for the discharge coefficient of the TPK_3 side weir is 17% and 7.2% higher than that of the TPK_1 and TPK_2 side weirs, respectively. The increase in the C_{dw} value of TPK_3 side weirs is justified by a reduction in the upstream angle and an increase in the upstream crest length so that a more significant portion of the crest length contributes to passing the flow. More optimum use of the upstream crest length can be achieved by reducing the upstream angle to facilitate the outflow over the side weir, which can be seen in the type of TPK_3 side weir. In contrast, the verticality of the upstream crest length of the TPK_1 (maximum upstream angle in this study) detaches the flow from the wall of the side weir.

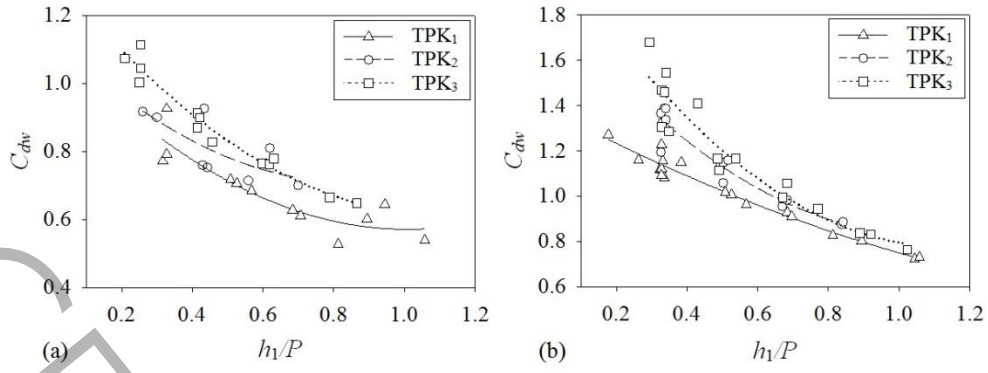

Fig. 3 variation of C_{dw} versus h_1/P for TPK_1, TPK_2, and TPK_3 side weirs: (a) P = 16 cm, L/W = 1.89; (b) P = 12 cm, L/W = 2.6

The hydraulic performance of the TPK_1 and TPK_3 side weirs with the same crest length and the different ranges of Froude numbers is compared in Fig. 4. Note that the length of the foundation (B_b) and the overhang length (B_i) in both geometries of triangular side weirs (TPK_1 and TPK_3) are the same size, which increases the advantage of these types of side weirs. As shown in Fig. 4(a), the flow in the dead zone doesn't pass over the upstream crest length of the TPK_1 side weir. However, the flow passes uniformly over the entire crest length of the TPK_3 side weir for lower Froude numbers (($F_1 \leq 0.3$) shown in Fig. 4(b). Also, as the Froude number increases ($F_1 > 0.3$), a circular zone of water containing different eddies forms upstream of the first cycle in two types of side weirs, which is more expanded in TPK_1. The eddy current, especially in high Froude numbers, happens due to decreasing the deflection angle of the lateral flow at the upstream of the side weir. In the case of TPK_1 Fig. 4(c), because of the vertical upstream crest length, this eddy is stronger than the TPK_3 Fig. 4(d). On the other hand, there is an area of flow interference between the two cycles, which expands due to a high disturbance [35]. In this area, the local suppression between the two cycles is also more severe for TPK_1 than TPK_3 side weir with the same water head. The flow disturbance due to the interference area in TPK_3 Fig. 4(d) is lower than the TPK_1 Fig. 4(c) side weir.

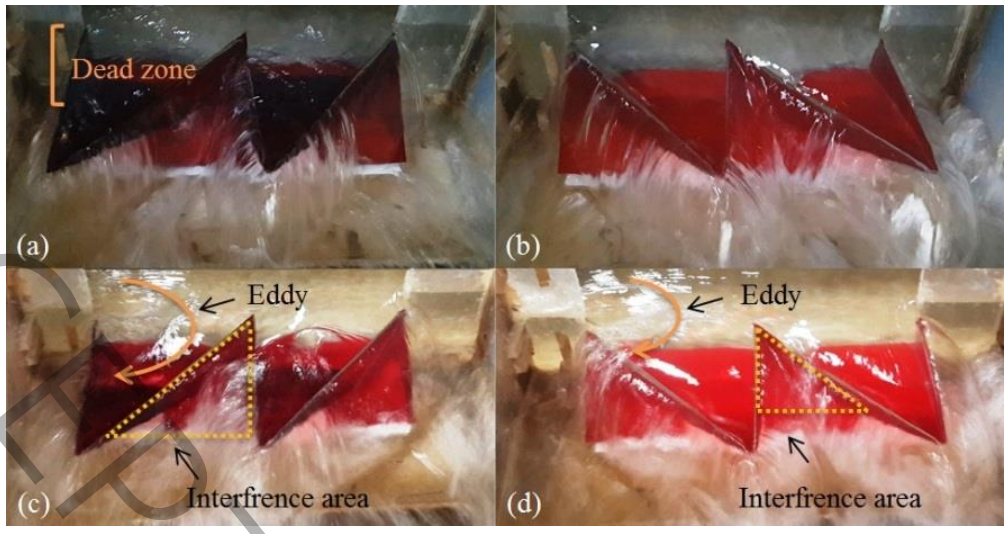

Fig. 4 Flow over triangular piano key side weirs: (left) TPK_1, (right) TPK_3, (a and b) $F_1 \leq 0.3$; (c and d) $F_1 > 0.3$

The effect of h_1/P on the discharge coefficient of triangular piano key and linear side weirs for the measured data is shown in Fig. 5. Regardless of the L/W ratio, C_{dw} is significantly more tremendous for triangular side weirs than for the linear side weirs. For a constant value of h_1/P, significant growth occurs in C_{dw} due to the increased crest length of the side weirs (L/W). The average discharge coefficient value for the triangular piano key side weirs with L/W = 3.35 is 1.5 to 3.46 times larger than linear side weirs. The impact of L/W significantly decreases for values of $h_1/P > 1$. All triangular side weirs' performance deteriorates after reaching the high head ($h_1/P > 1$) because of flow submerge in this descending part. Experiments were conducted at three different heights (P); therefore, the changes in the h_1/P parameter mainly depend on the alterations of h_1. The descending trend of the discharge coefficient versus h_1/P for triangular piano key side weirs is similar to frontal trapezoidal PK weirs [28] and rectangular PK side weirs [32]. The dispersion of data is attributed to the effect of the Froude number and other effective parameters.

Considering the studied flow behavior, the TPK_2 and TPK_3 side weirs can thus be regarded as more efficient designs than the TPK_1 side weirs. Therefore, the behavior and effective parameters in the TPK_2 and TPK_3 side weirs are compared in the following sections.

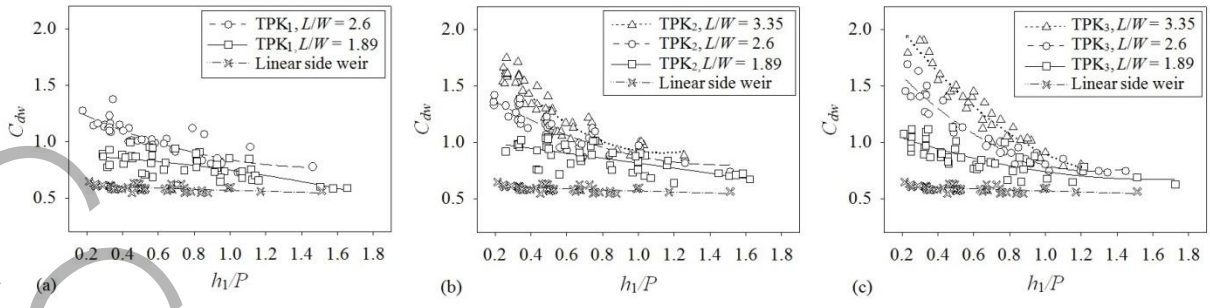

Fig. 5 Variation of C_{dw} versus h_1/P for linear and triangular side weir with different crest lengths: (a) TPK_1; (b) TPK_2; (c) TPK_3

Fig. 6 shows the effect of the Froude number at the upstream end (F_1) and downstream end (F_2) on the discharge coefficient of TPK_2 and TPK_3 side weirs with the same crest length (L/W = 1.89). It can be seen that the discharge coefficient increases by increasing the Froude number at the upstream and downstream end of the side weir for L/W = 1.89. Note that the increasing and decreasing influence of the Froude number on C_{dw} is generally attributed to the crest shape and the ratio of the opening length to the main channel width ([10, 18]). The secondary motion can alter the variation of the discharge coefficient against the Froude number. Considering the amounts of R^2 in Fig. 6, a more acceptable correlation exists between the discharge coefficient of triangular side weirs and F_2. Regarding the ranges of Froude number in this study ($F_1 < 0.77$ and $F_2 < 0.45$), a better correlation between F and C_{dw} may be observed for small ranges of this parameter.

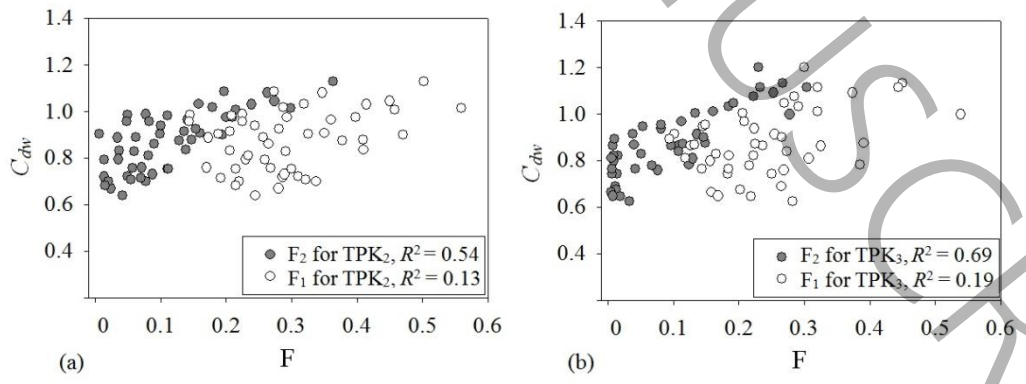

Fig. 6 Variation of C_{dw} versus F with L/W = 1.89: (a) TPK_2; (b) TPK_3

The effect of the Froude number at the downstream end on the discharge coefficient of TPK_2 with the different crest lengths has been revealed in Fig. 7. Increasing the amount of L/W leads to an increase in

the discharge coefficient of TPK_2. The results of R^2 indicate that the scatter in the values of C_{dw} in the side weirs with higher dimensionless weir lengths (L/W= 3.35, 2.6) is more remarkable. The scatter observed in the data values shows the sensible influence of the other parameters on the discharge coefficient. The tested results for two other side weirs (TPK_1 and TPK_3) also indicated the increasing trend of discharge coefficient with Froude number at the downstream end.

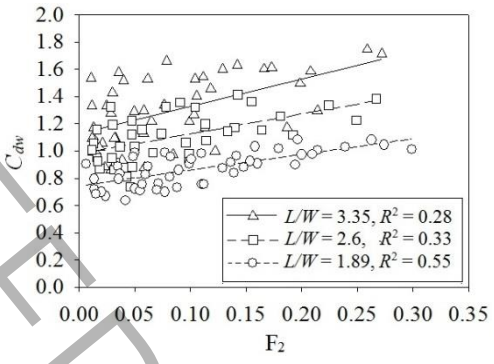

Fig. 7 Variation of C_{dw} versus F_2 for TPK_2 side weir with different L/W

The dimensionless parameters $\eta = Q_w/Q_1$ and $\chi = 1/F_2 \times y_2/P$ were studied to evaluate outflow efficiency, with F_2 and y_2 being the Froude number and the depth at the downstream end of the side weir, respectively. These parameters for a linear side weir have also been suggested [14]. For a better correlation between η and χ, the head over the side weir at the end of downstream ($h_2 = y_2 - P$) was considered. Fig. 8 represents the values of η versus χ for the TPK_2 and TPK_3 compared to linear side weirs. The figure indicates that the outflow efficiency for triangular side weirs is higher than that for linear ones. The changes in outflow efficiency would be attributed to the different crest lengths of the TPK side weirs compared with the linear ones. It is observed from Fig. 8 that the η rises when the ratio of χ increases. It can be explained that for constant values of h_2/P, lowering the F_2 leads to reducing the dynamic effect in the flow of the main channel. A similar trend was observed for rectangular piano key side weirs in a straight channel [32] and linear side weirs in a converging channel [14].

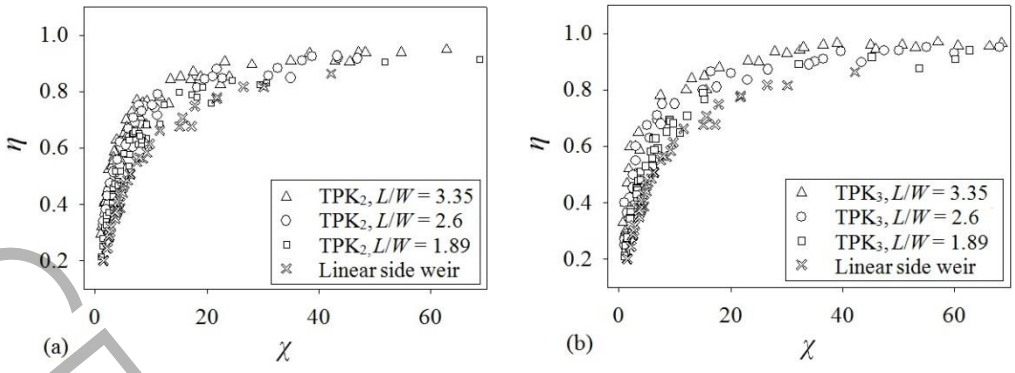

Fig. 8 η versus χ for TPK and Linear side weirs: (a) TPK_2; (b) TPK_3

The velocity components of the flow in the main channel affect the value of the deflection angle. The deflection angle of the lateral flow calculated by $\theta = \tan^{-1}(-V_z/V_x)$ in the present study is shown in Fig. 2. The increase of θ is a function of the growth in the value of $-V_z$, and the fall in the value of V_x, respectively [40]. In contrast, the flow toward the side weir is contracted by decreasing θ, and the diverted discharge declines over the side weir. Fig. 9 indicates the deflection angle at the channel bottom ($0.2y$) for TPK_2 and TPK_3 with specifications of P = 8 cm, L/W = 1.89, and F_2 = 0.07, 0.2, and 0.3. As shown in Fig. 9, the values of the deflection angle are low at upstream and downstream of the side weirs regardless of the shapes of the side weirs. Fig. 9 also indicates that the Froude number significantly affects the deflection angle, so increasing the Froude number decreases the value of θ and the side weir outflow. The collision of the flow observed at the connection point of the cycles leads a part of the flow to return to the main channel, and as a result, the values of θ at the middle of the side weir drop. It also follows from comparing the two types of side weirs that the TPK_2 with a higher upstream angle (δ_1/δ_2) creates lower values of θ compared with the TPK_3 side weir with the same crest length in the vicinity of the side weir, especially for the second cycle.

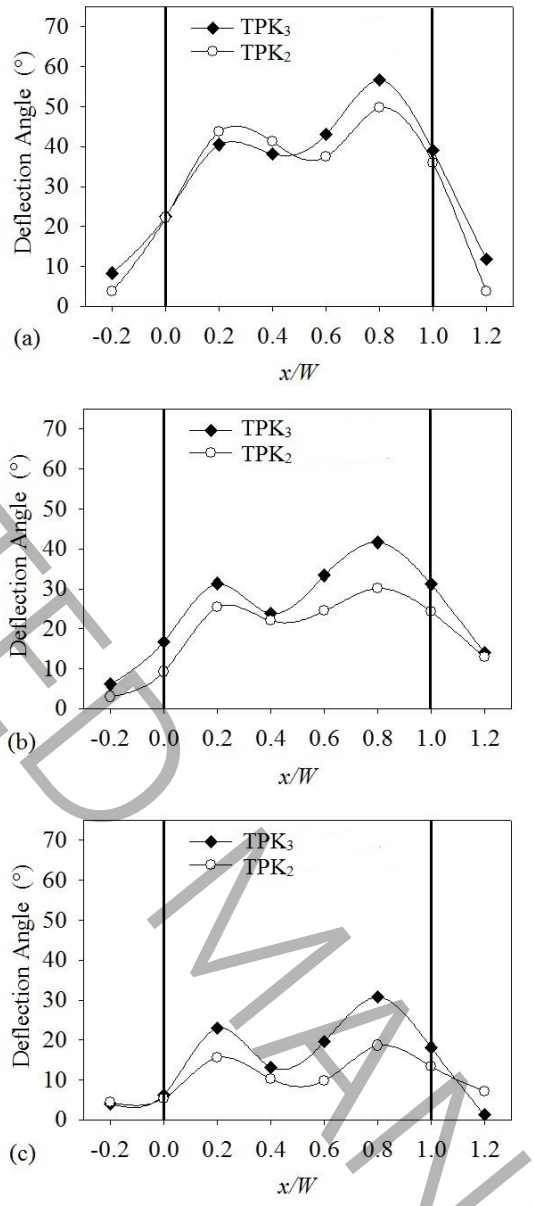

Fig.9 Variation of the deflection angle along the TPK_2 and TPK_3 side weirs at the channel bottom (0.2*y*) with *P* = 8 cm, *L*/*W* = 1.89: (a) F_2 = 0.07; (b) F_2 = 0.2; (c) F_2 = 0.3

Table 2 accurately describes the variation in deflection angle for TPK_1, TPK_2, and TPK_3 side weirs at two different points (first and second cycles of the TPK side weirs). The deflection angle values are more significant in the two proposed sections in the axis of *Z*/*b* = 0 at the first cycle (*x*/*W* = 0.2) and second cycle (*x*/*W* = 0.8) than in other sections near the side weirs. In this study, the ratio of variation in deflection angle (θ_{ij}) was defined as $\theta_{ij} = \theta_{TPKj} / \theta_{TPKi}$. According to the definition of θij, the values larger than one represent more diverted flow for TPK_j than TPK_i side weirs. The data analysis

highlights that the values of θij of the TPK_2 side weirs are higher than those of the TPK_1 side weirs and higher in TPK_3 than those of the TPK_2 side weirs.

Table 2. The ratio of variation in deflection angle (θ_{ij}) for TPK side weirs at the first and second cycles (z/b = 0)

TPK side weir	**Geometric and hydraulic specifications**			**First cycle(x/W = 0.2)**	**Second cycle(x/W = 0.8)**
Model	P(cm)	L/W	F_1	θ_{ij}= TPK_j/TPK_i	
TPK_2/TPK_1	8	1.89	0.40	۰/۸۱	۰/۹۲
TPK_2/TPK_1	8	2.6	0.35	۱/۱۲	۱/۱۲
TPK_2/TPK_1	12	1.89	0.35	۱/۳۶	۱/۳۰
TPK_2/TPK_1	12	2.6	0.28	۱/۵۰	۱/۶۱
TPK_2/TPK_1	16	1.89	0.18	۱/۲۲	۱/۲۴
TPK_2/TPK_1	16	2.6	0.20	۱/۴۰	۱/۴۷
TPK_3/TPK_2	8	1.89	0.45	۱/۱۱	۱/۰۲
TPK_3/TPK_2	8	2.6	0.51	۱/۱۱	۱/۲۱
TPK_3/TPK_2	8	3.35	0.48	۱/۲۰	1.28
TPK_3/TPK_2	12	1.89	0.32	۱/۲۱	۱/۲۱
TPK_3/TPK_2	12	2.6	0.40	۱/۲۳	۱/۳۰
TPK_3/TPK_2	12	3.35	0.32	۱/۳۴	۱/۴۲
TPK_3/TPK_2	16	1.89	0.22	۱/۱۴	۱/۱۹
TPK_3/TPK_2	16	2.6	0.18	۱/۵۰	۱/۶۰
TPK_3/TPK_2	16	3.35	0.22	۱/۵۰	۱/۶۶

Based on the study of the existing data and the parameters affecting the discharge coefficient of TPK side weirs, a regression equation can be defined as:

$$C_{dw} = 0.59\left(\frac{h_1}{P}\right)^{-0.18}\left(\frac{h_1}{B_i}\right)^{-0.14}\left(\frac{L}{W}\right)^{0.39}\left(\sin\left(\frac{\delta_1}{\delta_2}\right)\right)^{0.19}\left(\mathrm{F}_2\right)^{-0.01} \quad (10)$$

The robustness of our regression equation has been rigorously tested. We applied the equation to 70% of the data for estimation and the remaining 30% for validation. The results, presented in Table 3, showcase the estimated values for the standard error for each measured parameter, further affirming the reliability of our findings.

The error indices (R^2 = coefficient of determination, *RMSE* = root mean square error, and *MAE* = mean absolute error) were used for Eq. (10) to evaluate the precision of the nonlinear equation. R^2, *RMSE*, and *MAE* for Eq. (10) are 0.91, 0.065, and 0.052 considering 70% of the experimental data. Fig. 10(a) demonstrates that most extracted C_{dw} values from Eq. (10) have estimated measured C_{dw} values of TPK_1, TPK_2, and TPK_3 side weirs with acceptable accuracy within a $\pm$10% range. The derived discharge (Q_w) using the discharge coefficient has been estimated in this section, as shown in Fig.

10(b). The figure shows the measured values of Q_w against the estimated values for three types of TPK side weirs. The acceptable accuracy within a $\pm$10% range for TPK side weirs also was shown in Fig. 10(b).

Table 3. Estimated values for the exponents and error for the measured variables

		95% Confidence Interval	
Parameter	**Std.**	**Lower Bound**	**Upper Bound**
h_1/P	0.029	-0.238	-0.123
h_1/B_i	0.037	-0.215	-0.070
L/W	0.049	0.240	0.435
$\mathrm{Sin}(\delta_1/\delta_2)$	0.052	0.086	0.291
F_2	0.006	-0.022	0.003

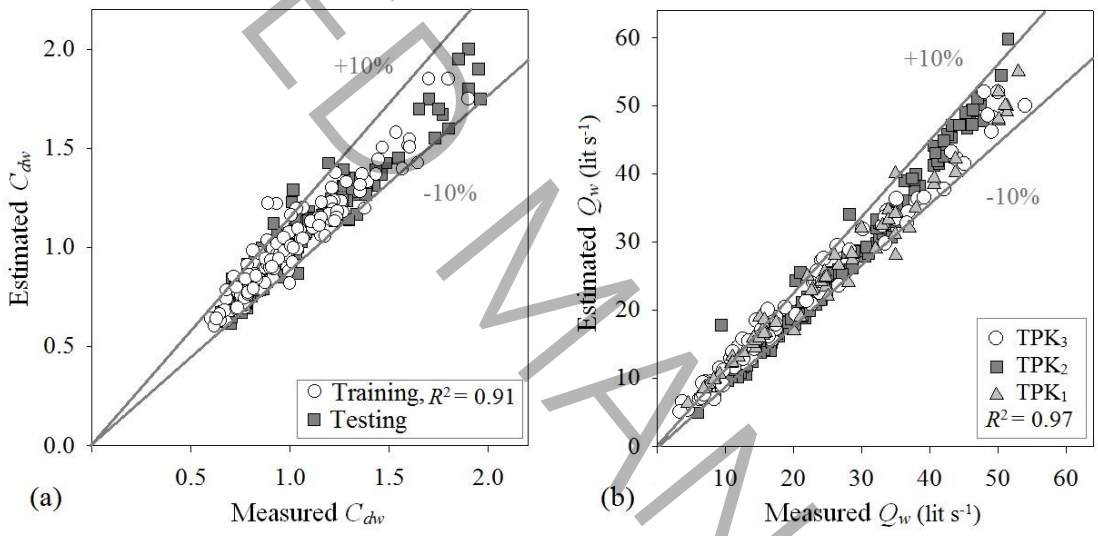

Fig. 10 Measured versus Estimated values (Eq. (10)) for TPK side weirs: (a) C_{dw}; (b) Q_w

Fig.11 represents the study results of C_{dw} versus h_1/P for piano key side weirs with different geometries. The results of the present and previous studies [32, 34] have been compared. Regardless of the geometry of side weirs, similar behavior of C_{dw} versus h_1/P is shown in Fig.11. For nearly the same amounts of L/W, the C_{dw} of triangular piano key side weirs is higher than trapezoidal and rectangular side weirs. It is believed that higher values of C_{dw} result from the triangular plan form proposed in the present study. As mentioned before, the hydraulic performance of the triangular piano key side weirs is improved by changing the geometry of TPK_2 to TPK_3.

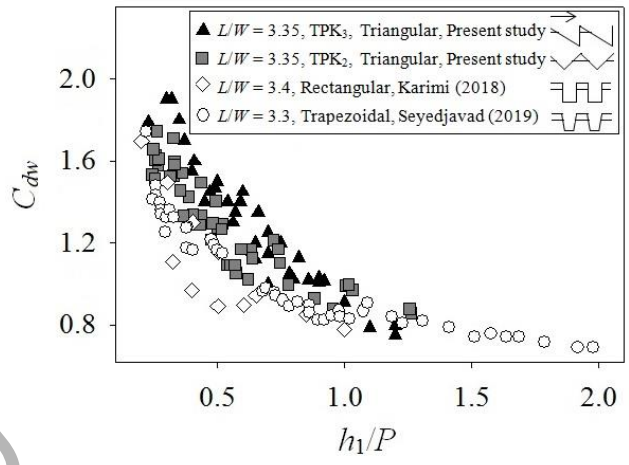

Fig. 11 Comparison of C_{dw} versus h_1/P for piano key side weirs in the present and previous studies

6. Conclusion

This experimental study, which is of significant importance in the field of hydraulic engineering, compares the discharge coefficient of the linear and triangular piano keys (TPK_1, TPK_2, and TPK_3) side weirs. The standard weir equation estimated by De Marchi was applied to evaluate the discharge coefficient in all tested side weirs. The ratio of the upstream angle (δ_1/δ_2), the length of the base (B_b), and the length of the overhang (B_i) are the main geometric differences between triangular piano key side weirs with the same crest length (L). The main findings of this study are as follows:

- In subcritical flow conditions, the acceptable average values of specific energy reduction were measured as 1.4%, 1.3%, and 1.2% for TPK_1, TPK_2, and TPK_3, respectively.
- The comparison between triangular piano key side weirs reveals the superior performance of the TPK_3. It demonstrates an average improvement of 17 % and 7.2 % higher than that of the TPK_1 and TPK_2 side weirs, respectively, in terms of C_{dw}.
- The discharge coefficient of triangular piano key side weirs with $L/W = 3.35$ and $0.2 < h_1/P < 1$ was up to 1.5 and 3.46 times larger than the linear side weirs, respectively.
- Due to the configuration of the upper crest, the eddies formed in the vicinity of the triangular piano key side weirs were more severe for TPK_1 than for TPK_3.
- Increasing the Froude number decreases the value of the deflection angle. TPK_2 side weir with a higher upstream angle (δ_1/δ_2) and the same crest length creates lower values of the deflection

angle compared with the TPK_3 side weir in the vicinity of the side weir, especially for the second cycle.

- A novel nonlinear equation, based on dimensionless parameters, is proposed for calculating the C_{dw} of the triangular piano key side weirs. This equation's prediction of the discharge coefficient was found to be satisfactory with R^2, *RMSE*, and *MAE* values of 0.91, 0.065, and 0.052, respectively. This innovative approach could significantly enhance the accuracy of C_{dw} calculations in future studies.
- Despite the better performance of TPK_3 side weirs, considering the smaller overhang length for TPK_3 compared to TPK_2, the former can be a better alternative in places with limited foundation lengths.
- Comparing the results of the present study with those previous studies indicates a similar behavior of C_{dw} versus h_1/P. However, the values of C_{dw} for triangular piano key side weirs are higher than those for rectangular and trapezoidal types for nearly the same amounts of L/W.

Nomenclature

A	Cross-sectional area of the flow, m^2
B	Upstream-downstream length of triangular piano key side weir, m
B_b	Base length, m
B_i	Overhang length, m
b	Width of the channel, m
C_{dw}	Discharge coefficient estimated by the opening length
E	Specific energy, m
F	Froude number
g	Acceleration of gravity, m/s^2
h	Head of water over the side weir crest, m
L	Side weir crest length, m
P	Side weir height, m
Q	Discharge in the main channel, m^3/s
Q_w	Diverted discharge over side weir, m^3/s
S_0	Bottom slopes
S_f	Friction slopes

V Mean flow velocity of the side weir, m/s

W Width of the side weir along the channel bank, m

W_i Width of the input cycle, m

W_o Width of the output cycle, m

x Distance from the beginning of the side weir, m

y Vertical direction from bottom, m

z Transverse distance from side weir, m

y Water depth in the main channel centerline, m

Greek symbols

δ Upstream angle, degrees

θ Deflection angle of the lateral flow

α Kinetic energy correction coefficient

σ Surface tension, N/m

ρ Mass density of the fluid, kg/m^3

μ Dynamic viscosity of the fluid, kg m^{-1} s^{-1}

Subscript

1 upstream section

2 downstream section

REFERENCES

[1] R. Daneshfaraz, R. Norouzi, P. Ebadzadeh, S. Di Francesco, J.P. Abraham, Experimental study of geometric shape and size of sill effects on the hydraulic performance of sluice gates, Water, 15(2) (2023) 314.

[2] R.H. French, R.H. French, Open-channel hydraulics, McGraw-Hill New York, 1985.

[3] W.H. Hager, P.U. Volkart, Distribution channels, Journal of Hydraulic Engineering, 112(10) (1986) 935-952.

[4] D. Marchi, Saggio di teoria del funzionamento degli stramazzi laterali (Theoretical knowledge on the functioning of sideweirs, L'Energia Elettria, 11(11) (1934) 849-860.

[5] K. Subramanya, S.C. Awasthy, Spatially varied flow over side-weirs, Journal of the Hydraulics Division, 98(1) (1972) 1-10.

[6] K.G.R. Raju, S.K. Gupta, B. Prasad, Side weir in rectangular channel, Journal of the Hydraulics Division, 105(5) (1979) 547-554.

[7] W.H. Hager, Lateral outflow over side weirs, Journal of Hydraulic Engineering, 113(4) (1987) 491-504.

[8] S. Borghei, M. Jalili, M. Ghodsian, Discharge coefficient for sharp-crested side weir in subcritical flow, Journal of Hydraulic engineering, 125(10) (1999) 1051-1056.

[9] A. Shariq, A. Hussain, M.A. Ansari, Lateral flow through the sharp crested side rectangular weirs in open channels, Flow Measurement and Instrumentation, 59 (2018) 8-17.

[10] H. Agaccioglu, Y. Yüksel, Side-weir flow in curved channels, Journal of irrigation and drainage engineering, 124(3) (1998) 163-175.

[11] A. El-Khashab, K.V. Smith, Experimental investigation of flow over side weirs, Journal of the Hydraulics Division, 102(9) (1976) 1255-1268.

[12] T. Honar, A. Keshavarzi, Effect of rounded-edge entrance on discharge coefficient of side weir in rectangular channels, Irrigation and Drainage: The journal of the International Commission on Irrigation and Drainage, 58(4) (2009) 482-491.
[13] A. Keshavarzi, J. Ball, Discharge coefficient of sharp-crested side weir in trapezoidal channel with different side-wall slopes under subcritical flow conditions, Irrigation and drainage, 63(4) (2014) 512-522.
[14] A. Maranzoni, M. Pilotti, M. Tomirotti, Experimental and numerical analysis of side weir flows in a converging channel, Journal of Hydraulic Engineering, 143(7) (2017) 04017009.
[15] A.S. Ramamurthy, L. Carballada, K. Subramanya, Uniformly discharging lateral weirs, Journal of the Irrigation and Drainage Division, 104(4) (1978) 399-412.
[16] M.R. Namaee, M.S. Jalaledini, M. Habibi, S.R.S. Yazdi, M.G. Azar, Discharge coefficient of a broad crested side weir in an earthen channel, Water Science and Technology: Water Supply, 13(1) (2013) 166-177.
[17] S.M. Borghei, M.A. Nekooie, H. Sadeghian, M.R.J. Ghazizadeh, Triangular labyrinth side weirs with one and two cycles, in: Proceedings of the Institution of Civil Engineers-Water Management, Thomas Telford Ltd, 2013, pp. 27-42.
[18] M.E. Emiroglu, N. Kaya, H. Agaccioglu, Discharge capacity of labyrinth side weir located on a straight channel, Journal of irrigation and drainage engineering, 136(1) (2010) 37-46.
[19] A. Kabiri-Samani, S.M. Borghei, H. Esmaili, Hydraulic performance of labyrinth side weirs using vanes or piles, in: Proceedings of the Institution of Civil Engineers-Water Management, Thomas Telford Ltd, 2011, pp. 229-241.
[20] A. Parvaneh, S. Borghei, M. Jalili Ghazizadeh, Hydraulic performance of asymmetric labyrinth side weirs located on a straight channel, Journal of irrigation and drainage engineering, 138(8) (2012) 766-772.
[21] H.Z. Khameneh, S.R. Khodashenas, K. Esmaili, The effect of increasing the number of cycles on the performance of labyrinth side weir, Flow measurement and instrumentation, 39 (2014) 35-45.
[22] F. Nezami, D. Farsadizadeh, M.A. Nekooie, Discharge coefficient for trapezoidal side weir, Alexandria Engineering Journal, 54(3) (2015) 595-605.
[23] M. Karimi, M.J. Ghazizadeh, M. Saneie, J. Attari, Flow characteristics over asymmetric triangular labyrinth side weirs, Flow Measurement and Instrumentation, 68 (2019) 101574.
[24] R. Daneshfaraz, R. Norouzi, J. Patrick Abraham, P. Ebadzadeh, B. Akhondi, M. Abar, Determination of flow characteristics over sharp-crested triangular plan form weirs using numerical simulation, Water Science, 37(1) (2023) 211-224.
[25] A. Schleiss, From labyrinth to piano key weirs: A historical review, in: Proc. Int. Conf. Labyrinth and Piano Key Weirs Liège B, 2011, pp. 3-15.
[26] M. Karimi, M. Jalili Ghazizadeh, M. Saneie, J. Attari, Experimental and numerical study of a piano key side weir with oblique keys, Water and Environment journal, 34 (2020) 444-453.
[27] R. Anderson, B. Tullis, Piano key weir hydraulics and labyrinth weir comparison, Journal of Irrigation and Drainage Engineering, 139(3) (2013) 246-253.
[28] A. Mehboudi, J. Attari, S. Hosseini, Experimental study of discharge coefficient for trapezoidal piano key weirs, Flow Measurement and Instrumentation, 50 (2016) 65-72.
[29] F. Alizadeh Sanami, M.H. Afshar, M. Saneie, Experimental study on the discharge coefficient of triangular piano key weir, Irrigation and Drainage, 71(2) (2022) 333-348.
[30] O. Machiels, S. Erpicum, B.J. Dewals, P. Archambeau, M. Pirotton, Experimental observation of flow characteristics over a Piano Key Weir, Journal of hydraulic research, 49(3) (2011) 359-366.
[31] A.T. Le, K. Hiramatsu, T. Nishiyama, Hydraulic comparison between piano key weir and rectangular labyrinth weir, GEOMATE Journal, 20(82) (2021) 153-160.
[32] M. Karimi, J. Attari, M. Saneie, M.R. Jalili Ghazizadeh, Side weir flow characteristics: comparison of piano key, labyrinth, and linear types, Journal of Hydraulic Engineering, 144(12) (2018) 04018075.
[33] A. Saghari, M. Saneie, K. Hosseini, Experimental study of one-and two-cycle trapezoidal piano-key side weirs in a curved channel, Water Supply, 19(6) (2019) 1597-1603.

[34] M. Seyedjavad, S.T.O. Naeeni, M. Saneie, Laboratory investigation on discharge coefficient of trapezoidal piano key side weirs, Civ Eng J, 5(6) (2019) 1327-1340.
[35] M. Yeganeh, M.J. Ghazizadeh, M. Saneie, E. Zeighami, Comparison of Hydraulic Performance of Triangular Side Weirs with a Focus on the Overhang Type, KSCE Journal of Civil Engineering, 27(10) (2023) 4263-4273.
[36] S. Balahang, M. Ghodsian, Evaluating performance of various methods in predicting triangular sharp-crested side weir discharge, Applied Water Science, 13(9) (2023) 171.
[37] F. Henderson, 1966, Open channel flow, Macmillan, New York.
[38] S. Erpicum, B.P. Tullis, M. Lodomez, P. Archambeau, B.J. Dewals, M. Pirotton, Scale effects in physical piano key weirs models, Journal of Hydraulic Research, 54(6) (2016) 692-698.
[39] P. Novák, J. Čabelka, Models in hydraulic engineering: Physical principles and design applications, Monographs & surveys in water resources engineering, (1981).
[40] S. Bagheri, M. Heidarpour, Characteristics of flow over rectangular sharp-crested side weirs, Journal of Irrigation and Drainage engineering, 138(6) (2012) 541-547.